



Evaluating Petrographic and Mechanical Property Correlations in Sihapas Formation for High-Pressure Hydraulic Fracturing Using Pearson and Spearman Methods

Budi Prayitno¹, Daffa Akhillah¹, Novrianti Novrianti², Dike Fitiransyah² and Dedikarni Panuh³

¹Department of Geological Engineering, Faculty of Engineering, Universitas Islam Riau
Kaharuddin Nasution Street No. 113 Perhentian Marpoyan, Pekanbaru, Riau, 28284, Indonesia.

²Department of Petroleum Engineering, Faculty of Engineering, Universitas Islam Riau,
Kaharuddin Nasution Street No. 113 Perhentian Marpoyan, Pekanbaru, Riau, 28284, Indonesia.

³Department of Mechanical Engineering, Faculty of Engineering, Universitas Islam Riau
Kaharuddin Nasution Street No. 113 Perhentian Marpoyan, Pekanbaru, Riau, 28284, Indonesia.

Corresponding author: Budi Prayitno (budiprayitno@eng.uir.ac.id)

Manuscript received: January 19th, 2026; Revised: February 09th, 2026

Approved: February 12th, 2026; Available online: March 13th, 2026; Published: March 13th, 2026.

ABSTRACT - This study aimed to evaluate the suitability of natural frac sand (SiO₂) from the Sihapas Formation as a proppant for hydraulic fracturing in unconventional oil and gas reservoirs in Riau Province, Indonesia. Quantitative–qualitative evaluation in hydraulic fracturing systems is conducted to assess the performance of quartz grains (SiO₂) in enhancing and maintaining fluid flow conductivity under the influence of stress, formation blockage, and chemical interactions. Sieve distribution analysis was performed to determine particle size distribution, crush resistance testing was conducted to evaluate mechanical strength, and X-Ray Diffraction (XRD) was used to characterize mineral composition. The correlative relationships among parameters were further analyzed using Pearson and Spearman statistical methods, with API RP 56 (frac sand) and API 19C (proppant) standards serving as benchmarks. The results showed that the 40/70 mesh fraction dominates across samples, though roundness values fall below specification thresholds while sphericity remains within acceptable ranges. Grain hardness testing at 5000 psi showed relatively high destruction rates, while mineralogical analysis confirmed a consistently high SiO₂ composition (≥98%) with secondary clay minerals. Elevated turbidity and alkaline pH values were also observed. Statistical analysis showed strong correlations among parameters, reflecting the influence of geological transport processes on grain morphology and mineral decomposition due to diagenetic processes. In general, these findings showed that natural frac sand samples do not fully meet API standards, highlighting the need for innovation and direct well testing to enhance material quality for hydraulic fracturing applications.

Keywords: fracturing, hydraulic, conductivity, silica, proppant, sihapas.

How to cite this article:

Budi Prayitno, Daffa Akhillah, Novrianti Novrianti, Dike Fitiransyahand Dedikarni Panuh, 2026, Evaluating Petrographic and Mechanical Property Correlations in Sihapas Formation for High-Pressure Hydraulic Fracturing Using Pearson and Spearman Methods, Scientific Contributions Oil and Gas, 49 (1) pp. 187-203. DOI org/10.29017/scog.v49i1.1999.

INTRODUCTION

Hydraulic fracturing is a widely applied well-stimulation technique used to enhance oil and gas production, particularly in reservoirs characterized by inherently low permeability and porosity. (Zoveidavianpoor & Gharibi, 2015), In this process, a high-pressure fracturing fluid is injected into the reservoir through the wellbore, inducing the formation to crack and thereby creating new fractures or extending existing ones. These fractures serve as conduits that facilitate the flow of hydrocarbons towards the wellbore, thereby improving production efficiency (Al-Muntasheri 2014).

The integrity of fractures (Al-Muntasheri 2014) is maintained by introducing proppants into the fluid to ensure that fractures remain open. Proppants are granular materials introduced into the newly created fractures to maintain fracture conductivity by preventing closure once the pumping pressure is reduced. The selection of proppant type is a key determinant of the success of hydraulic fracturing. As the properties of proppant types, such as their mineral composition, grain size, shape, and mechanical strength, directly affect the long-term productivity of the fractured reservoir (Lam 2019; Hamzah et al., 2021)

The performance of proppants is evaluated through a series of well-established standards, primarily defined by the American Petroleum Institute (API Standard 19C SECOND EDITION 2018) and the International Standards Organization (ISO). Key proppant characteristics include particle size, roundness, sphericity, crush resistance, acid solubility, bulk density, absolute density, and turbidity. These properties are interrelated and collectively determine the efficiency of fracture conductivity and the stability of the proppant under reservoir conditions.

Particle size is directly correlated with the ability of the proppant to withstand closure stress. Larger particles typically show higher crush resistance, while smaller particles tend to disintegrate under high pressures (Tang et al., 2018). Crush resistance testing is essential for determining a proppant's ability to withstand closure pressures representative of subsurface conditions (Bestaoui 2014). This property is particularly important in deep wells where closure pressures can be exceedingly high. The shape characteristics of proppants, such as sphericity and roundness, influence the packing behavior of proppant particles within fractures. Proppant sphericity and roundness significantly influence crush resistance and conductivity (Kamel et al., 2019). The following is presented to calculate the sphericity factor, providing a measure of the degree to which a proppant particle approximates the geometry of an ideal Equaion 1:

$$\Psi_v = \frac{v}{d_v a_g} \quad (1)$$

where d_v is the mean volume diameter and a_g the specific surface area determined by the laser granulometer. The next phase of the hardness evaluation is computed according to the following Equation 2:

$$m_p = 24.7 \times \rho_{\text{bulk}} \quad (2)$$

where ρ is the bulk density. Equation (3) calculates the amount of crushed material as a percentage of the mass of proppant sample recovered from the cell (m'_{pan}):

$$m'_{\text{pan}} = \frac{m_{\text{pan}}}{m_s} \times 100 \quad (3)$$

where m'_{pan} is the mass of fines generated in the test, m_s is the mass of proppant recovered from the cell, and m'_{pan} is the weight percent of fines generated in the crush test. This is attributed to the wider distribution area of stress (Zoveidavianpoor & Gharibi 2016). Higher fracture conductivity can be achieved through improved proppant packing efficiency when particles exhibit greater sphericity and roundness (Bose et al., 2015). The relationship is particularly significant because conductivity, defined as the product of permeability and pack width, is directly influenced by proppant size and shape (R.D. Barree 2003; Richard et al., 2019). High sphericity and roundness improve the permeability of the proppant pack, allowing for an efficient flow of hydrocarbons through the fracture network.

Grains exhibiting a high degree of roundness show reduced angularity, thereby minimizing proppant pack compaction and maintaining higher fracture conductivity throughout the operational lifespan of the well. These shape parameters are rigorously tested according to ISO 13503-2 standards, which ensure that the proppants contribute effectively to fracture permeability. Acid solubility is another important parameter that measures the extent to which proppants may dissolve in acidic conditions, often present during stimulation treatments. High acid solubility shows the presence of impurities, which can weaken the proppants mechanical integrity and negatively affect fracture conductivity (Xu et al., 2022). ISO 13503-2 specifies a maximum solubility threshold of 2% for sand and resin-coated proppants if greater than or equal to 30/50 mesh and 3% for smaller proppants. This ensures that the materials maintain sufficient stability under reactive conditions.

Bulk density and absolute density are essential in determining the weight and the resultant proppant transportability through the fracturing fluid. Proppant density influences the rheological behavior and transport capacity of the fracturing fluid, thereby affecting the efficiency of proppant placement within newly created fractures. Turbidity is a key quality indicator because high levels of fine particulate matter can cause flowback and productivity issues, thereby reducing the

effectiveness of the hydraulic fracturing treatment (Ahmed et al., 2017).

Silica sand with nearly pure SiO_2 content, rounded grains, high crush resistance, uniform size, and low oxide content shows superior quality and is suitable as a proppant in hydraulic fracturing to keep fractures open and enhance the permeability of low-permeability reservoirs (Ahmed et al., 2017; Wahab Gaber et al. 2021), Mississippi (Lam 2019), Malaysia (Saa'id et al., 2011) and Indonesia (Effendi & Firdaus 2023) have been explored for their silica resources. However, a major limitation of natural silica sands is their limited capacity to withstand the high closure pressures typical of deep well environments (Tschapek et al., 1983). When proppants lack sufficient mechanical strength to withstand formation closure stresses, crushing may occur, resulting in the generation of fine particles. These fines may clog the pore spaces within proppants pack, significantly reducing fracture conductivity (Bestaoui-Spurr 2014).

The use of high-quality proppants offers a strategic approach to minimizing environmental impacts by improving the efficiency of cleaner gas production in low-permeability reservoirs, thereby supporting emission reduction targets (Syaranamual et al., 2025).

METHODOLOGY

Geology regional and field sampling

The geology of the investigation area is administratively located in several districts in Riau Province. The sample selection is determined based on geological characteristics and the accessibility of sampling locations. The sample selection is generally carried out on rock bodies/formations that are considered to meet the predetermined criteria. The distribution of silica sandstone consists of the Minas Formation, Sihapas Formation, Lalat Formation, Muara Enim Formation, and Gumai Formation. The geomorphology of the landform of the survey area generally consists of steep to moderately low undulating structural hills at varying heights between low-medium hills (10-50 meters above sea level), medium-high hills (51-87 meters above sea

level), and high hills (177-344 meters above sea level). As shown in Figure 1, the lithological analysis indicates that the Sihapas Formation exhibits a dominant rock distribution and relatively favorable grain characteristics.

The sample selection process was conducted with precision, taking into account the geological characteristics and sediment particle properties that may qualify as potential proppant materials. The samples were systematically collected from several strategic sites within the Sihapas and Minas Formations. These formations were selected based on their distinctive depositional environments, which offer a diverse range of grain sizes, mineralogical compositions, and other critical properties essential for optimizing hydraulic fracturing performance.

The Sihapas Group (Bekasap Formation and Bangko Formation), characterized by its high quartz content and well-sorted sandstones, presents an ideal source for proppant material. Similarly, the Minas Formation, characterized by distinct depositional environments and mineralogical properties, presents a diverse range of sediment types that may satisfy established proppant specifications. These geological features provided an eclectic selection of samples that represent different sedimentary facies, ensuring a comprehensive evaluation of their suitability as proppants. The Sihapas Group on the Bekasap Formation was formed in an estuarine environment within a complex of channels and sand bars, with a thickness of ± 501.28 meters (Herdiansyah et al., 2023).

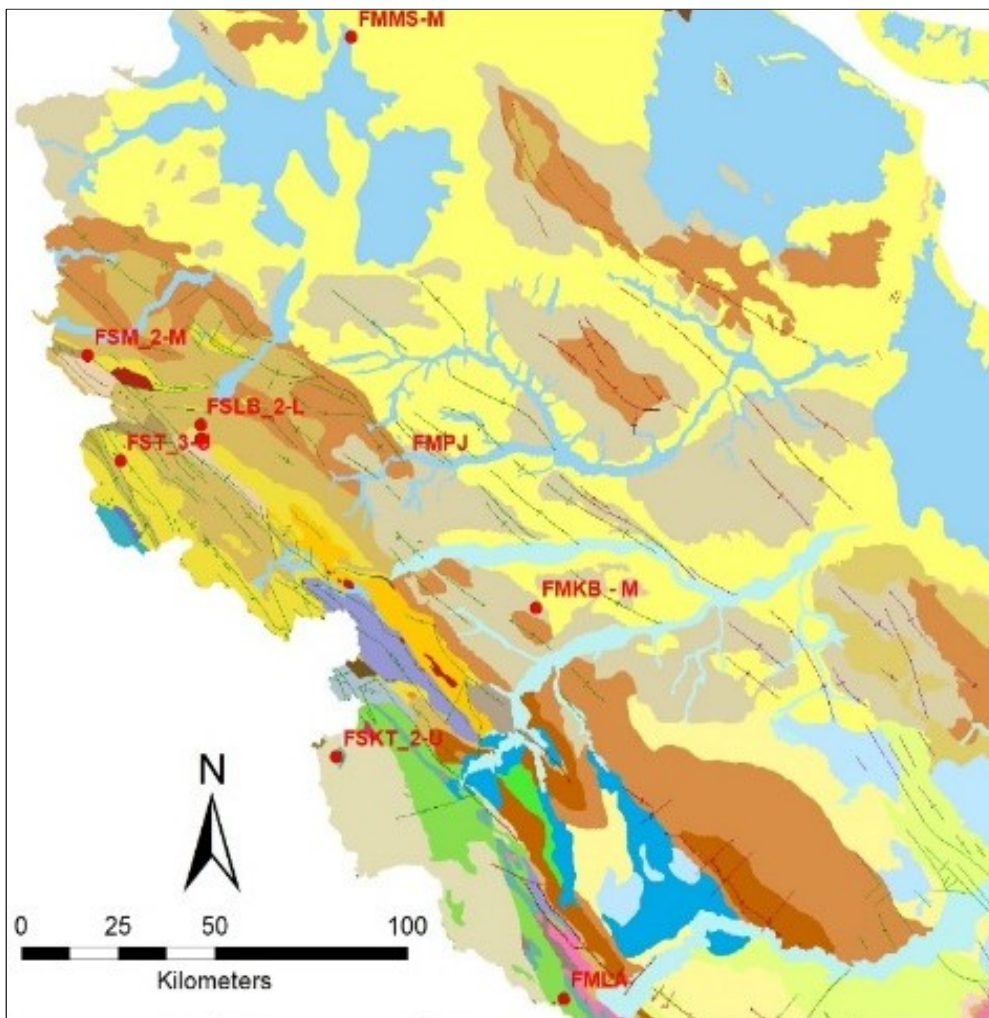


Figure 1a. Map of selected natural frac sand distribution from various geological formations in several regencies in the Riau Province - Indonesia. This study focuses on the sihapas formation (yellowish-brown) and the minas formation (light gray).

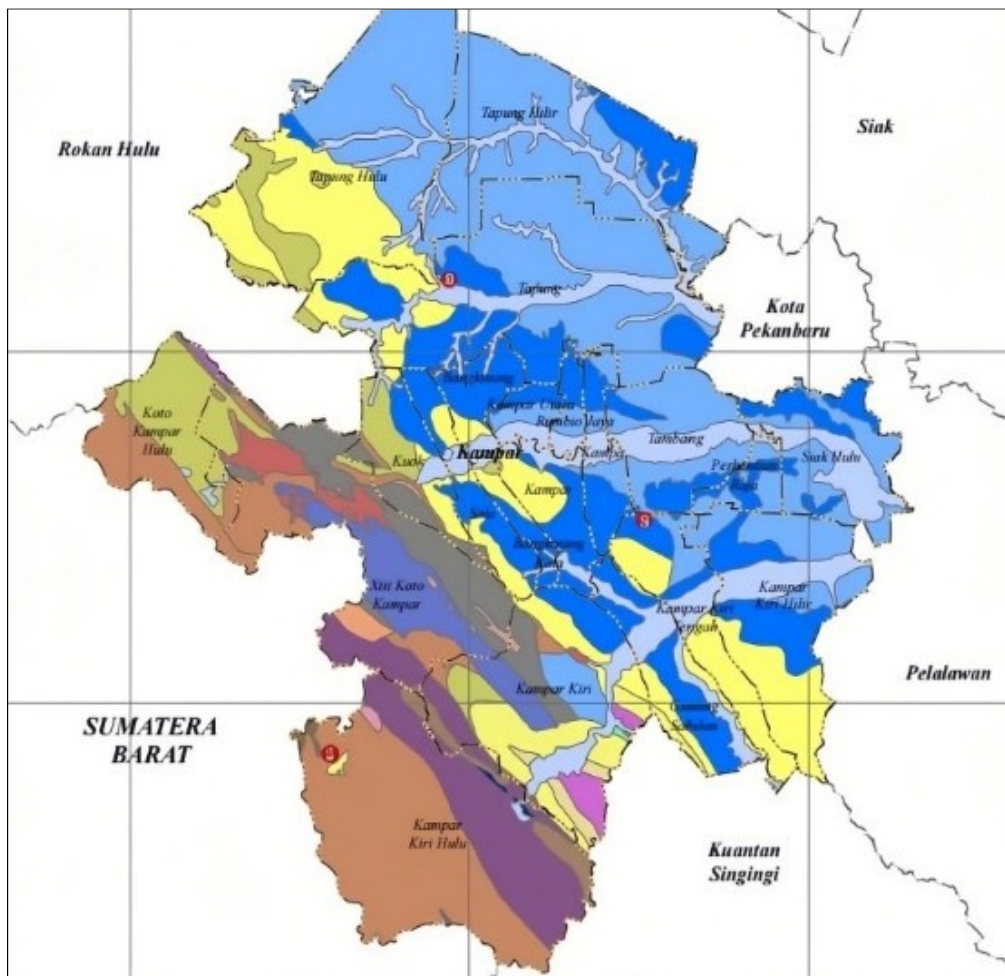


Figure 1b. Distribution map of sample locations FSKT_2 upper (1), FMKB_middle (2), and FMPJ (3).

Measurement and laboratory analysis

Laboratory testing was carried out at the Testing Center for Oil and Gas LEMIGAS, adhering to the standards set by the American Petroleum Institute (API), specifically API RP 56 for frac sand and API 19C for proppant materials. These internationally recognized protocols are essential for ensuring that analytical procedures meet industry standards. In addition, evaluated samples must comply with the stringent specifications required for hydraulic fracturing operations. The laboratory analysis focused on four key parameters: (1) grain size distribution through sieve analysis, (2) physical properties including sphericity and roundness, (3) crush resistance to assess mechanical strength under pressure, and (4) mineralogical composition determined using X-Ray Diffraction (XRD).

To explore the relationships between physical and chemical variables, statistical correlation analyses were conducted using both Pearson's and Spearman's methods, providing insights into the interdependence of material characteristics relevant to proppant performance.

Figure 2 shows a flowchart for testing of frac sand natural samples according to API RP 56 and API RP 19C Standards for Hydraulic Fracturing Applications. XRD and crush resistance testing were conducted after the grain distribution testing. The sieve analysis was conducted to determine the particle size distribution of the sand samples. This step is important because the size of proppants particle directly impacts fracture conductivity. The particles must be uniform and within a specific size range. The typical proppants are defined in (ASTM-E11 2017, Table 1). The calibrated sieve is

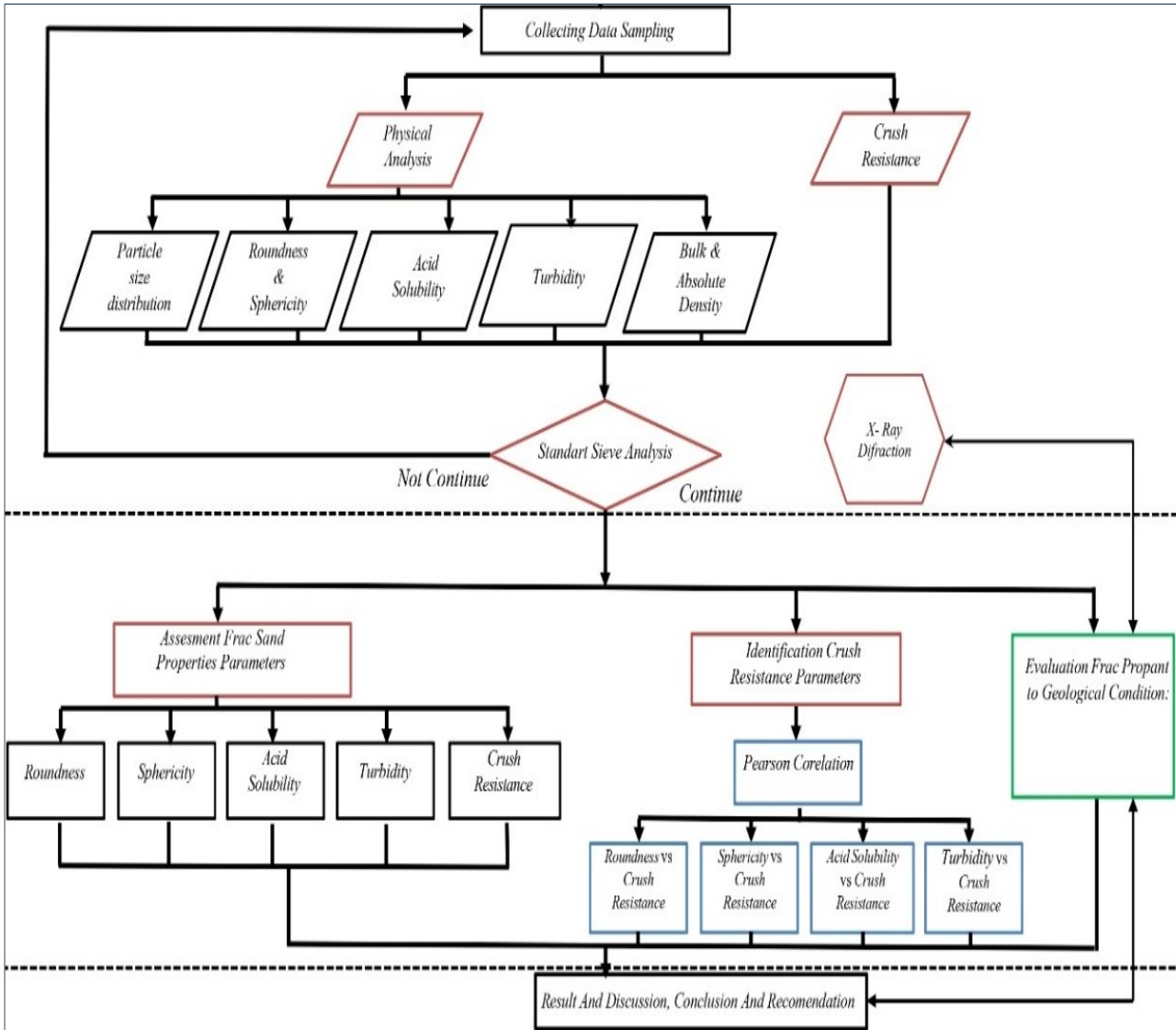


Figure 2. Flowchart for testing of frac sand natural sampel according to API RP 56 and API RP 19C standards for hydraulic fracturing applications.

arranged sequentially according to the recommended method, i.e., (API RP 56, 58, and 19C 2008 & ISO 13503-2-2006 & Mark, 2007) to ensure they can effectively prop open fractures without excessive compaction or migration. The calibrated sieves were arranged in a specific sequence, and samples were agitated using a Ro-Tap shaker to determine the weight distribution across different size classes. Several previously weighed sand samples are loaded into the top sieve. The sieve stack is placed in a Ro-Tap Shaker and shaken for 10 minutes. Then, the number of samples in each sieve is measured, and the percentage weight is calculated according to Figure 3.

Physical properties

Roundness and sphericity

The physical characteristics of the particles, particularly roundness and sphericity, were assessed using the Krumbein and Sloss scales. Roundness measures the smoothness of particle edges, while sphericity indicates how closely the particles resemble a spherical shape. Both attributes significantly influence the uniform packing behavior of proppants within fractures and the maintenance of high permeability. High roundness and sphericity reduce the risk of particle interlocking and promote better flow of

Evaluating Petrographic and Mechanical Property Correlations in Sihapas Formation for High-Pressure Hydraulic Fracturing Using Pearson and Spearman Methods (Prayitno et al.)

Table 1. Results of grain size distribution analysis. The grain size distribution of the samples indicates the dominant size fraction in the mesh 40/70 range (FSM_2 middle and FST_3 upper) and 70/140 range (FSM_2 lower and FSKT_2 upper). At size 70/140 is preferable as a proppant based on the API RP 19C specification, whereas at 40/70 range is preferable for frac sand applications based on the API RP 56 specification.

| Mesh Number And Particel Size in (μm) <i>inchi</i> | FSM_2 (Middle) | FMT_3 (Upper) | FSLB_1 (Upper) | FSLB_2 (Upper) | FSLB_2 (Lower) | FMPJ - | FMMS (Middle) | FMKB (Middle) | |
|--|-------------------|------------------|-------------------|-------------------|-------------------|-----------|------------------|------------------|-------|
| 12 | (1700) 0.0661 | 0.00 | 0.13 | 0.11 | 0.01 | 0.21 | 1.90 | 1.25 | 0.14 |
| 14 | (1400) 0.0555 | 0.01 | 0.34 | 0.19 | 0.05 | 0.51 | 2.35 | 1.81 | 0.21 |
| 16 | (1200) 0.0473 | 0.03 | 0.69 | 0.25 | 0.06 | 0.62 | 2.23 | 1.84 | 0.35 |
| 18 | (1000) 0.0394 | 0.07 | 1.05 | 0.43 | 0.07 | 0.70 | 2.12 | 2.20 | 1.44 |
| 20 | (850) 0.0331 | 0.04 | 0.70 | 0.28 | 0.01 | 0.27 | 2.39 | 1.78 | 0.75 |
| 25 | (710) | 0.12 | 1.64 | 0.82 | 0.05 | 0.76 | 3.13 | 3.22 | 3.40 |
| 30 | (560) 0.022 | 0.31 | 2.51 | 1.80 | 0.19 | 1.18 | 3.70 | 7.51 | 6.08 |
| 35 | (500) | 0.83 | 3.86 | 2.81 | 0.51 | 1.93 | 5.02 | 9.39 | 8.09 |
| 40 | (425) 0.016 | 1.54 | 5.15 | 9.01 | 0.84 | 2.48 | 6.19 | 7.79 | 9.57 |
| 45 | (355) | 6.45 | 8.97 | 10.69 | 3.26 | 8.13 | 7.98 | 9.81 | 13.52 |
| 50 | (300) | 8.00 | 16.16 | 13.15 | 13.51 | 10.70 | 10.33 | 10.31 | 14.69 |
| 60 | (250) 0.01 | 11.70 | 20.61 | 14.52 | 35.33 | 11.58 | 10.03 | 9.12 | 12.85 |
| 70 | (210) 0.0083 | 19.57 | 16.86 | 16.21 | 25.06 | 14.27 | 9.94 | 8.13 | 9.47 |
| 80 | (165) 0.0065 | 22.86 | 7.29 | 14.00 | 10.18 | 21.18 | 7.20 | 5.48 | 4.53 |
| 100 | (149) 0.0059 | 13.84 | 4.01 | 9.19 | 5.87 | 13.55 | 5.41 | 3.97 | 2.95 |
| 120 | (125) 0.0049 | 5.40 | 1.86 | 3.22 | 1.62 | 4.42 | 2.98 | 2.42 | 2.17 |
| 140 | (105) 0.0041 | 0.36 | 0.06 | 0.12 | 0.00 | 0.01 | 0.29 | 0.03 | 0.22 |
| 170 | (88) 0.0031 | 4.22 | 3.54 | 2.24 | 2.23 | 2.98 | 3.56 | 4.34 | 2.49 |
| Pan | 0 | 4.61 | 4.19 | 0.76 | 1.14 | 1.87 | 1.97 | 7.89 | 6.60 |
| US STD Mesh 20/40: 0.42 – 0.84 mm (coarse – medium sand) | | | | | | | | | |
| Mesh 40/70: 0.21 – 0.42 mm (fine - medium sand) | | | | | | | | | |
| Mesh 70/140: 0.105 – 0.21 mm (very fine – fine sand) | | | | | | | | | |

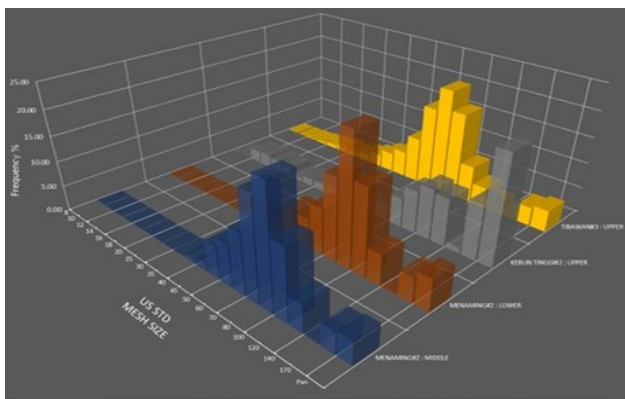


Figure 3. (a) Results of grain size distribution analysis. The literacy studi results show that the Sihapas Formation has a dominant rock distribution and quite good grain characteristics. (b) One of the sampling locations at FSKT_2 upper on Sihapas Formation.

hydrocarbons through the proppant pack. The degree of roundness measures the grain angle's relative sharpness or the grain's curvature. The degree of particle polishing (*sphericity*) measures how close the sand particles approach the shape of

a ball. These two parameters were observed under a binocular microscope and calculated by point-counting, referring to scales, the (*Krumbein, W. C., & Sloss, L. L., 1963*). *Stratigraphy and Sedimentation (2 Ed)*. *Freeman, 1963*) (Figure 4).

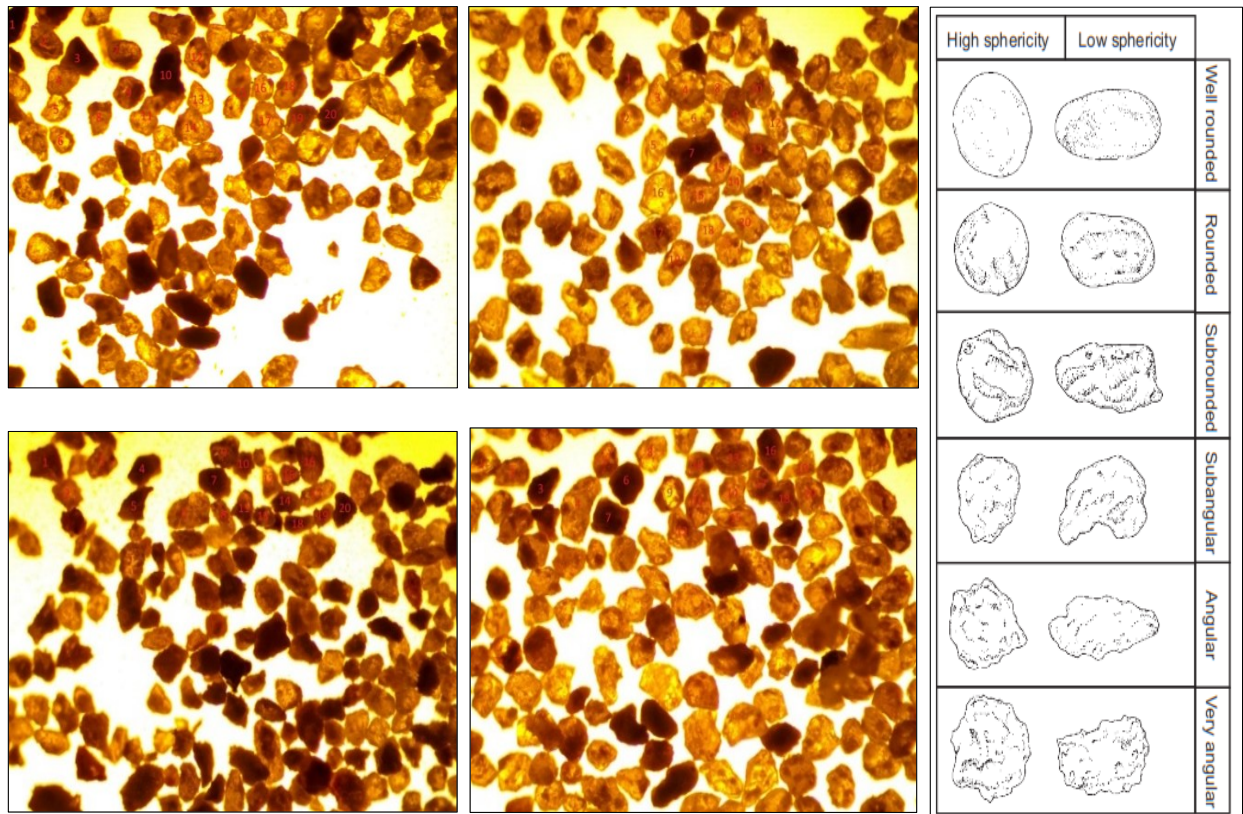


Figure 4. Photomicrograph of natural frac sand by X-ray Diffraction (XRD). (a) top-left: FSM_2 Middle average roundness 0.3 and average sphericity 0.6 (b) top-right: FSM_2 Lower average roundness 0.3 and average sphericity 0.6 (c) FSKT_2 Upper :bottom-left: average roundness 0.3 and average sphericity 0.5 and (d) FST_3 Upper: bottom-right average roundness 0.3 and average sphericity 0.6 (Krumbein & Sloss 1963; Pettijhon et al 1987).

Density

Bulk density testing measures the weight per unit volume, including voids and sand pores. This test determines the amount of sand required to fill a fracture or reservoir. Absolute density testing determines the density of a particle by incorporating its internal porosity into the total volume measurement. This test uses a low-viscosity liquid that wets the particles' surfaces.

Turbidity

Turbidity is a measure of the amount of suspended fine material present in the proppant. High turbidity values indicate the presence of fine particulate contaminants, which can lead to increased formation damage and reduced fracture conductivity. None of the samples met the acceptable turbidity limits, indicating potential issues with the presence of impurities or insufficient processing. Table 2

Crush resistance

The crush resistance tests were performed to evaluate the mechanical strength of the proppants sample under high closure stresses, which are typical in deep reservoir environments. During hydraulic fracturing, the closure pressure exerted by the formation can be extremely high, and only proppants with sufficient crush resistance can prevent fracture closure and maintain flow paths for hydrocarbons. The samples were subjected to incremental pressures, and the percentage of particles crushed at each pressure level was measured. This test helps determine whether proppants can withstand the compressive forces encountered in the subsurface without breaking down into fines that could impair permeability. The test helps compare the sand crush resistance and overall strength under various pressures (4.500 ~ 5.000 psi). Sand samples are pressed with varying pressure levels, and the percentage of destruction

according to API RP 56 and 19C methods. Table 2 and Table 3. Chemical Properties.

X-ray diffraction (XRD)

XRD analysis was conducted to determine the mineralogical composition of the samples, focusing primarily on the identification and quantification of quartz, clay minerals, and other components. Quartz is a desirable component owing to its hardness and chemical stability, characteristics that make the mineral highly suitable as a proppant material. However, the presence of clays or other reactive minerals can adversely affect the performance of proppants by reducing their crush resistance or increasing their solubility in acidic conditions. The XRD results provided insights into the overall quality of the samples and their suitability for high-pressure fracturing environments.

XRD analysis is a rapid method used for the identification of the mineral phases in a sample. This method is particularly suitable for fine-grained sediments where polarizing microscopy would have difficulty distinguishing the individual phases of minerals. This test uses an automatic Rigaku SmartLab X-ray diffractometer (9kW) with a 1D High-Speed detector and an Ultrafast D/tex detector. First, the selected sample is washed using

toluene to remove oil and other contaminants. The washed samples are then dried and ground into a powder measuring <0.062 mm. Furthermore, the powder is placed and flattened into the sample holder, ready for sequential analysis.

The presence of a particular mineral is qualitatively determined by comparing the recorded diffractogram with a reference to the mineral standard in a pre-installed powder diffraction database. The proportions of each mineral are estimated semi-qualitatively (in percentage by weight) based on their peak intensity by a reference procedure elaborated by several researchers, and empirical matrix corrections are applied for normalization.

Spearman correlation (ρ), Pearson correlation (R) analysis

The surface properties of proppants materials, including roundness, turbidity, sphericity, and acid solubility, exhibit a significant correlation with crush resistance, which is important for determining the effectiveness of proppants in maintaining fracture conductivity under high closure pressures. A rigorous statistical analysis was conducted to explore the underlying causes of poor compressive strength observed in the crush

Table 2. Frac Sand Properties test result table on eight natural quartz sand samples based on API RP 56 and API RP 19-C testing standards and specifications.

| Test Parameter | Unit | API RP 56 | API RP 19C | FSM_2 (Middle) | FMT_3 (Upper) | FSLB_1 (Upper) | FSLB_2 (Upper) | FSLB_2 (Lower) | FMPJ - | FMMS (Middle) | FMKB (Middle) |
|-----------------------------------|-------------------|---|------------|----------------|---------------|----------------|----------------|----------------|---------------|---------------|---------------|
| Dominant size distribution | % | UNS | UNS | 40/70 (45.71) | 40/70 (62.61) | 40/70 (54.56) | 40/70 (77.16) | 40/70 (44.68) | 40/70 (38.28) | 40/70 (37.36) | 40/70 (50.53) |
| Roundness | K&S | ≥ 0.6 | ≥ 0.6 | 0.3 | 0.3 | 0.2 | 0.3 | 0.2 | 0.3 | 0.2 | 0.3 |
| Sphericity | scale | ≥ 0.6 | ≥ 0.6 | 0.6 | 0.6 | 0.6 | 0.6 | 0.6 | 0.6 | 0.7 | 0.7 |
| Acid Solubility | % | ≤ 2 | ≤ 3 | 2.003 | 1.577 | 6.454 | 11.392 | 7.724 | 3.082 | 12.071 | 30.461 |
| Bulk Density | g/cm ³ | UNS | UNS | 1.230 | 1.435 | 1.333 | 1.503 | 1.198 | 1.490 | 1.276 | 1.201 |
| Absolute Density | g/cm ³ | UNS | UNS | 2.683 | 2.672 | 2.680 | 2.670 | 2.682 | 2.684 | 2.675 | 2.681 |
| Turbidity | FTU | ≤250 | ≤250 | 6550 | 5925 | 9275 | 2925 | 8125 | 1400 | 600 | 2175 |
| pH Water | - | UNS | UNS | 8.68 | 8.68 | 8.73 | 8.73 | 8.73 | 8.73 | 8.73 | 8.73 |
| pH Water + Sand (Turbidity) | - | UNS | UNS | 7.22 | 7.46 | 7.51 | 7.50 | 8.32 | 7.90 | 7.28 | 7.02 |
| Crush Resistance 40/70 @5.000 psi | % fines | ≤ 8 | ≤ 10 | 64.04 | 27.80 | 52.61 | 29.61 | 85.38 | 28.92 | 39.83 | 29.08 |
| UNS: Unspecified specification | | XXXX : Does not meet suggested specification on both specification | | | | | | | | | |

Table 3. Table of crush resistance test results, related parameters, and their correlations on 8 samples analyzed at 40/70 grain fraction, the correlations marked in black letters use the Pearson formula (R), while those marked in blue (roundness and sphericity) use the Spearman formula (ρ). r is the correlation to crush resistance.

| Sample ID | | FSM_2 (Middle) | FMT_3 (Upper) | FSLB_1 (Upper) | FSLB_2 (Upper) | FSLB_2 (Lower) | FMPJ - | FMMS (Middle) | FMKB (Middle) | r |
|-------------------------------------|-------------------|-------------------|----------------------------------|-------------------|-------------------|----------------------------|-----------|------------------|------------------|--------|
| Roundness | K&S Scale | 0.3 | 0.3 | 0.2 | 0.3 | 0.2 | 0.3 | 0.2 | 0.3 | -0.573 |
| | ranked | 4 | 1 | 6 | 2 | 8 | 3 | 7 | 5 | 0.738 |
| Sphericity | K&S Scale | 0.6 | 0.6 | 0.6 | 0.6 | 0.6 | 0.6 | 0.7 | 0.7 | -0.298 |
| | ranked | 6 | 4 | 7 | 5 | 8 | 3 | 2 | 1 | 0.690 |
| Acid Solubility | % | 2.003 | 1.577 | 6.454 | 11.392 | 7.724 | 3.082 | 12.071 | 30.461 | -0.269 |
| Bulk Density | g/cm ³ | 1.230 | 1.435 | 1.333 | 1.503 | 1.198 | 1.490 | 1.276 | 1.201 | -0.633 |
| Absolute Density | g/cm ³ | 2.683 | 2.672 | 2.670 | 2.670 | 2.682 | 2.684 | 2.675 | 2.681 | 0.475 |
| Turbidity | FTU | 6550 | 5925 | 9275 | 2925 | 8125 | 1400 | 600 | 2175 | 0.681 |
| Quartz (XRD) | % | 97.00 | 98.00 | 93.00 | 98.00 | 92.00 | 100.00 | 96.00 | 72.00 | -0.796 |
| Crush | value | 64.04 | 27.80 | 52.61 | 29.61 | 85.38 | 28.92 | 39.83 | 29.08 | - |
| Resistance 40/70 @5.000 psi | ranked | 7 | 1 | 6 | 4 | 8 | 2 | 5 | 3 | - |
| Crush Resistance 40/70 @4.000 | ≤8 and ≤10 | - | 25.19 | - | - | - | - | - | - | - |
| | | 61.80 | 21.22 | - | - | - | - | - | - | - |
| | | 60.16 | - | - | - | - | - | - | - | - |
| | @3.000 | | | | | | | | | |
| | @1.500 | | | | | | | | | |
| Crush Resistance 70/140 @5.000 | ≤6 and ≤10 | 38.88 | - | - | - | - | - | - | - | - |
| | | 33.40 | - | - | - | - | - | - | - | - |
| | @5.000 | 24.36 | - | - | - | - | - | - | - | - |
| | @3.000 | | | | | | | | | |
| | @1.500 | | | | | | | | | |
| Note : ±0.5 – 1.0 (high corelation) | | | ±0.3 – 0.5 (moderate corelation) | | | ±0.0 – 0.3 (no corelation) | | | | |

resistance tests of the samples analyzed. Specifically, eight representative samples from the 40/70 grain size fraction were selected to ensure a proportional and comprehensive understanding of their characteristics across the dataset of ten samples.

To evaluate the correlation between crush resistance and other material properties, both Pearson's and Spearman's correlation analyses were used. Pearson's correlation coefficient (R) was used for continuous numerical data, while Spearman's rank correlation coefficient (\tilde{r}) was applied to ordinal and categorical data, such as roundness and sphericity.

These correlation methods provide insights into the interrelationships among key variables and their influence on proppant performance, as depicted in Table 3. The strength of the correlation was categorized as follows: ±0.0 to ±0.3, indicating negligible correlation, ±0.3 to ±0.5, suggesting moderate correlation, and ±0.5 to ±1.0, indicating a strong correlation. Figure 5.

RESULT AND DISCUSSION

The particle size distribution and rounding of proppant materials are largely determined by the geological origin of the source rock and the mechanical processes it undergoes over time. These characteristics develop mainly through prolonged physical weathering and subsequent transportation Khaing et al., 2022. The effective particle size reduction and enhancement in roundness result from the combined effects of chemical and mechanical weathering, further intensified by transportation through hydrodynamic (water), aeolian (wind), or gravitational forces Khaing et al., 2017. The combination of these processes contributes to the breakdown of larger rock masses into smaller, rounded particles suitable for use in hydraulic fracturing operations.

The transport processes of sedimentary particles play a crucial role in determining the final quality of proppant materials. In addition to transport dynamics, factors such as the lithology of the parent rock, its mineralogical composition, and its history of weathering and erosion directly influence

the degree of particle roundness and sphericity. Uniformity in particle morphology – commonly referred to as good sorting is typically a result of consistent and sustained sediment transport mechanisms. For example, sediment particles transported over long distances by fluvial systems or through aeolian processes are subjected to repeated collisions and abrasion against other particles and surfaces. The repetitive mechanical interactions gradually enhance the particles’ roundness and sphericity (Wahab Gaber et al., 2021b). These conditions promote the formation of high-performance proppants, characterized by consistent particle size, high roundness, and sphericity parameters essential for maintaining fracture conductivity and minimizing flow resistance in hydraulic fracturing operations (R.D. Barree, 2003) Quartz Content and Crush Resistance, X-ray Diffraction (XRD) analysis showed a strong negative correlation (-0.796) between the quartz content and the degree of grain crushing, as shown in Table 4.

Higher quartz concentrations in proppants enhance resistance to crushing forces. Quartz, being a hard and chemically stable mineral, improves the mechanical integrity of proppants under the extreme closure pressures typical of deep reservoirs. This finding emphasizes the necessity of maximizing quartz purity in proppant formulations to enhance durability and preserve fracture

conductivity. Outlier samples, such as FMKB_Middle, were excluded from the analysis to provide a more accurate representation of the overall trend, as shown in Table 2. Roundness and Sphericity: Roundness and sphericity were found to have strong positive correlations with crush resistance, with correlation coefficients of 0.738 and 0.690, respectively (Liu et al., 2024; Wei et al., 2022), (Ibrahim et al., 2025), as shown in Table 3.

This highlights the importance of particle shape in determining proppant performance (Ibrahim et al., 2025). High roundness reduces the number of angular contact points, which are susceptible to stress concentration and potential fracture. Similarly, increased sphericity promotes a more uniform stress distribution across particles, minimizing weak points and preventing premature failure. Proppants with superior roundness and sphericity not only enhance crush resistance but also improve fracture conductivity by minimizing interlocking and promoting efficient packing within the fracture. The poor roundness shows that the particles are largely angular and irregular, which severely affects their ability to pack efficiently within fractures. The angular particles can lead to increased stress concentrations, higher friction, and ultimately reduce the permeability of the proppant pack, undermining fracture conductivity and reducing well performance, as shown in Table 6.

Table 4. Summary of XRD analysis results

| Sampel ID | Clay mineral | | | Carbonate mineral | | | | Other mineral | | | | Total | | | |
|-----------|--------------|------|-------|-------------------|-----|-----|------|---------------|--------|-------|-----|-------|-----|-------|--------|
| | smt | ilts | ilt | kao | chl | cal | dlmt | sdr | qrt | p.fls | plg | gpy | pyt | cly | Othr |
| FSM_2M | - | - | 1,00 | 2,00 | - | - | - | - | 97,00 | - | - | - | - | 3,00 | 97,00 |
| FSM_2L | - | - | Tr | 1,00 | - | - | - | - | 99,00 | - | - | - | - | 1,00 | 99,00 |
| FSKT_2U | - | - | 10,00 | 13,00 | - | - | - | - | 77,00 | - | - | - | - | 23,00 | 77,00 |
| FST_3U | - | - | 2,00 | - | - | - | - | - | 98,00 | - | - | - | - | 2,00 | 93,00 |
| FSLB_1U | - | - | 1,00 | 6,00 | - | - | - | - | 93,00 | - | - | - | - | 7,00 | 93,00 |
| FSLB_2L | - | - | - | 2,00 | - | - | - | - | 98,00 | - | - | - | - | 2,00 | 98,00 |
| FSLB_3L | - | - | 1,00 | 5,00 | - | - | - | - | 92,00 | 2,00 | - | - | - | 2,00 | 94,00 |
| FMPJ | - | - | - | - | - | - | - | - | 100,00 | - | - | - | - | 0,00 | 100,00 |
| FMMS_M | - | - | tr | 4,00 | - | - | - | - | 96,00 | - | - | - | - | 4,00 | 96,00 |
| FMKB_M | - | - | 7,00 | 21,00 | - | - | - | - | 72,00 | - | - | - | - | 28,00 | 72,00 |

Note:
 Smt: smectite Ilts: Illite smectite Ilt: illite Chl:chlorite Dlmt: dolomite
 Sdr: siderite Kao: kaolinite Qrt: quartz cal: calcite p.fls: Potash Feldspar
 Pyt: pyrite Clay, tr: trace Plg: plagioclase Carbonate Mineral is absen

Roundness and sphericity are essential attributes, as both characteristics govern particle packing within fractures and the maintenance of permeability. High roundness minimizes sharp edges that can act as stress concentration points, thereby reducing the risk of particle crushing under high closure pressures. Sphericity ensures that the particles approximate a spherical shape, which allows for efficient packing and maximizes void space for fluid flow. The roundness and morphological shape of proppant particles play an important role in the determination of their ability to pack effectively within fracture apertures and maintain fluid permeability. High roundness helps minimize the presence of sharp edges on particle surfaces, which can serve as stress concentration points, thereby reducing the likelihood of particle crushing under elevated closure pressures, as shown in Tables 2 and 6.

Particles that exhibit a near-spherical shape promote uniform and efficient packing, which maximizes interparticle void space and enhances fluid flow through the proppant pack. The combined effect of good roundness and high sphericity is essential for preserving the long-term stability of fracture conductivity, particularly under cyclic loading and high-stress conditions in unconventional reservoirs. Crush resistance testing on the 40/70 grain size fraction showed that all

analyzed samples did not meet the maximum particle failure limits set by API RP 56 and API 19C, which are 8% and 10%, respectively.

The recorded percentage of failure exceeded the allowable tolerance threshold, indicating that the proppant material from the location has low mechanical strength under high closure stress. The high failure rate serves as a critical indicator that the proppant does not meet the specifications required for operational conditions demanding long-term mechanical stability. Fragile particles tend to produce a large quantity of fines, which can clog fluid flow paths within the fracture. The accumulation of these fine materials will reduce the effective permeability of the fracture system, decrease flow capacity, and ultimately reduce fracture conductivity. The efficiency of hydrocarbon production, especially in unconventional reservoirs, is highly dependent on the stability of fracture conductivity. Therefore, improving mechanical properties through particle modification is still urgently needed to ensure that fracture conductivity can be maintained properly (Ibrahim et al., 2025).

Friction during large-scale proppant injection processes affects the friction between the proppant and the wall rock along the fracture path, with both characteristics playing an important role in the efficiency of proppant distribution. Finer-grain

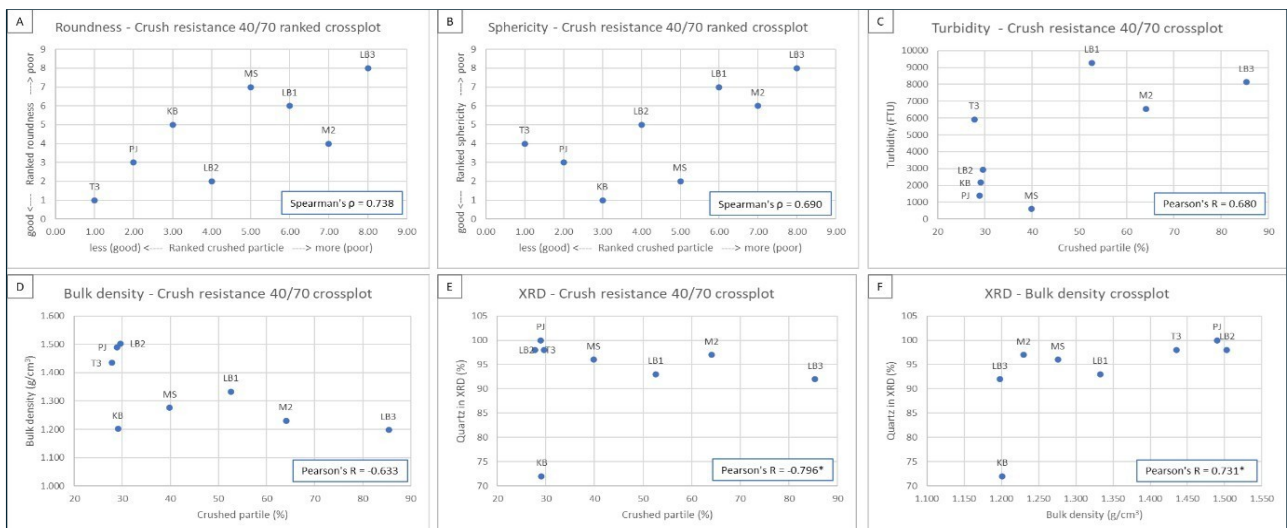


Figure 5. Crossplot of parameters that correlate with crush resistance results in grain fraction 40/70, crossplot with roundness and sphericity parameters (A & B) using ranking values with spearman correlation (ρ), while other crossplots (C, D, E, and F) use numerical values directly with Pearson correlation (R).

characteristics (well sorting) provide denser friction, causing proppant to settle around the well wall and reducing the effectiveness of fracture stimulation. Conversely, the interaction between proppant and the wall in poorly sorted grains creates additional turbulence, which reduces effective friction and increases horizontal proppant transport. This allows the proppant to remain suspended longer in the fracturing fluid and reach more distant fracture areas. Conductivity refers to the capacity of a formed fracture to transmit fluid from the reservoir to the production well (Ngwe et al., 2019; Peng et al., 2025)

Turbidity and crush resistance: Turbidity showed a strong positive correlation with crush resistance (0.681). High turbidity shows the presence of fine particulate contaminants or impurities, which tend to weaken the structural integrity of the proppant under pressure. These fines can reduce the mechanical strength of the proppant pack and produce debris that further compromises fracture conductivity. Therefore, reducing turbidity through enhanced processing and purification is important for improving the performance and longevity of proppant materials, as shown in Table 3.

Bulk density and crush resistance: bulk density exhibited a strong negative correlation with crush resistance (-0.633), indicating that proppants with lower bulk densities are more susceptible to crushing. Bulk density is a function of the mineral

composition of the sample, where a higher quartz content results in increased density and improved strength. This positive relationship between quartz content and bulk density suggests that increasing the proportion of durable minerals like quartz (2.65 ~ 2.66 g/cm³) while minimizing weaker constituents, such as clays (2.58 ~ 2.60 g/cm³), can enhance proppant resistance to closure pressure. This adjustment also supports the maintenance of fracture integrity under operational conditions. **Impact of Polycrystalline Quartz:** The analysis also highlighted a critical limitation related to the type of silica present.

The majority of the samples contained polycrystalline quartz, which is inherently weaker compared to monocrystalline quartz. The polycrystalline structure features multiple crystal boundaries that act as potential failure points under high pressure, thereby reducing the overall crush resistance. To improve the mechanical performance of the proppant, a shift toward monocrystalline quartz, which provides higher strength due to fewer internal weaknesses, may be necessary.

The X-ray diffraction (XRD) analysis shed light on the mineralogical composition of the samples. This shows that most samples were composed almost entirely of quartz (97-99 wt%), which is generally favorable for proppant use due to quartz's hardness and chemical stability. However, the FSKT_2 upper sample contained only 77% quartz, with a significant presence of clay minerals. The

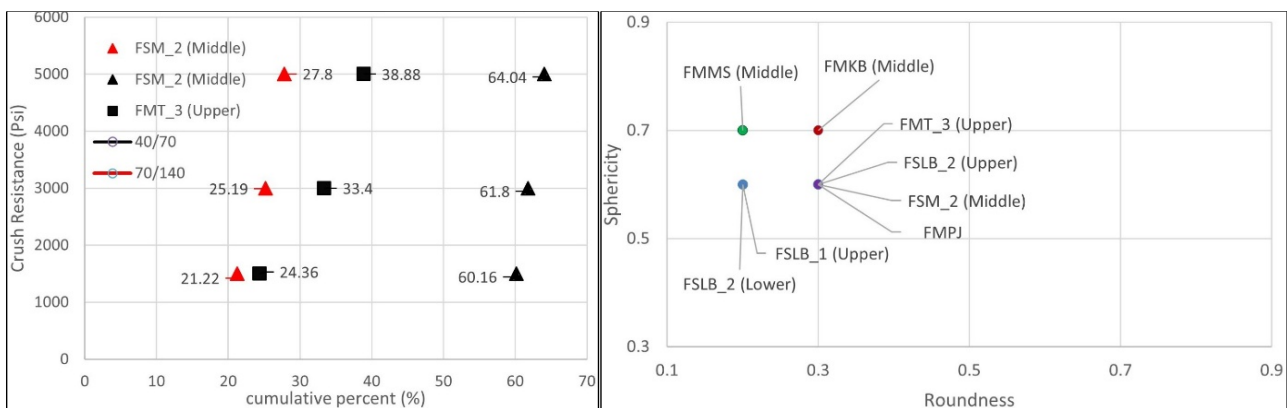


Figure 6. Crossplots of grain morphology (shape and size) against compressive strength test results for samples FSM_2 (Middle) and FMT_3 (Upper) demonstrate a consistent trend, marked by decreasing load capacity (Psi). Acid solubility plays a substantial role in reducing grain strength. Thus, the combined influence of morphological and chemical factors is critical in determining the mechanical performance of grains during compressive strength evaluation.

increased proportion of clay not only contributed to the higher turbidity and acid solubility but also weakened the structural integrity of the proppant. Clay minerals are known to be less resistant to crushing and chemically reactive, which negatively affects the performance of the proppant under both mechanical and chemical stresses. Figure 5 and Figure 6.

CONCLUSION

The analysis of roundness and sphericity for the samples showed considerable deficiencies, indicating their inadequacy for use as proppant materials under industry standards. The roundness of all the samples was rated at a visual scale of 0.3, which is significantly below the minimum requirement specified by API RP 56 and API 19C.

The acid solubility test results for all samples did not meet the specifications outlined in API RP 56 (Frac Sand) and API RP 19C (Proppant), indicating a high content of reactive minerals. Bulk density is a function of the mineral content and moisture level. The crush resistance test results at 5,000 psi for all samples did not meet the specifications set by API RP 56 (Frac Sand) and API RP 19C (Proppant). This showed that the proppant particles are highly susceptible to compressive stress, whether originating from formation pressure or injection-related loading. However, crush resistance performance improved in the 40/70 and 70/140 grain size fractions as the applied stress was reduced.

The advanced purification technologies and post-treatment processes are required to enhance the technical quality of the material's grains, particularly in terms of mechanical strength, and to reduce turbidity caused by the presence of contaminants. These refinement measures are important to ensuring that the material meets the technical standards required, especially regarding grain resistance under pressure loads typical in hydraulic fracturing applications. This study confirmed that proppant grains that do not meet mechanical strength standards lead to grain failure,

finer generation, and reduced fracture conductivity. As a proposal, this study is directed toward addressing stress load issues on mechanical strength through the innovative application of *nano-silica* fracturing fluids, which are expected to improve proppant distribution, enhance grain resistance, and sustain fracture conductivity efficiency.

ACKNOWLEDGEMENT

Gratitude was conveyed to the PT. PERTAMINA HULU ROKAN and the Directorate of Research and Community Service (DPPM) of Universitas Islam Riau for its financial support. We also extend our gratitude to LEMIGAS Jakarta for providing the laboratory facilities, which ensured the smooth operation of the sample testing. Finally, thanks to all parties involved in the research process, including survey and sample collection.

GLOSSARY OF TERMS AND SYMBOLS

| Terms & Symbols | Definition | Unit |
|------------------|--|------|
| US STD | a classification system used to determine the particle size of granular materials | |
| ISO 13503-2:2006 | International Standards Organization for evaluating proppants used in hydraulic fracturing | |
| FTU/NTU | Formazin/Nephelometric Turbidity Unit | |
| API | American Petroleum Institute | |
| ρ | Spearman correlation | |
| R | Pearson correlation | |
| SiO ₂ | <i>Silicon dioxide; Silicon (Si) Oxygen (O)</i> | |
| XRD | X-ray diffractometry analysis | |
| MPa | A megapascal is a unit of pressure | |

| | |
|-------|--|
| Psi | Pound per square inch unit of pressure |
| smt | smectite |
| ilts | illite smectite |
| ilt | illite |
| chl | chlorite |
| dlmt | dolomite |
| sdr | siderite |
| kao | kaolinite |
| qrt | quartz |
| cal | calcite |
| p.fls | potash feldspar |
| pyt | pyrite clay |
| tr | trace |
| plg | plagioclase |
| UNS | Unspecified specification |
| xxx | Does not meet suggested specification on both specifications |

REFERENCES

- Ahmed, H., Ismaiel, H., & Ali, A. I., 2017, Evaluation of White Silica Sands in the North Eastern Desert, Egypt. In Egypt Article in the International Journal of Scientific and Engineering Research. <https://www.researchgate.net/publication/317956531>
- Al-Muntasheri, G. A., 2014, A critical review of hydraulic-fracturing fluids for moderate- to ultralow-permeability formations over the last decade. *SPE Production and Operations*, vol. 29, no. 4, pp. 243–260. <https://doi.org/10.2118/169552-PA>
- API STANDART 19C SECOND EDITION., 2018. Measurement of and Specifications for Proppant Used in Hydraulic Fracturing and Gravel-pack Operations.
- Bestaoui, N., 2014, Materials Science Improves Silica Sand Strength. *SPE - European Formation Damage Conference, Proceedings, EFDC*, 1. <https://doi.org/10.2118/168158-MS>
- Bestaoui-Spurr, N., 2014, SPE 168158 Materials Science Improves Silica Sand Strength.
- Bose, C. C., Fairchild, B., Jones, T., Gul, A., & Ghahfarokhi, R. B., 2015, Application of nanopropants for fracture conductivity improvement by reducing fluid loss and packing of micro-fractures. *Journal of Natural Gas Science and Engineering* vol. 27 pp. 424–431. <https://doi.org/10.1016/j.jngse.2015.05.019>.
- Effendi, D., & Firdaus, A. N., 2023, Penggunaan Pasir Proppant Sebagai Media Hydraulic Fracturing Menggunakan Standar Api-Rp 19C vol. 4 no. 2. Oktober. <http://journal.itsb.ac.id/index.php/JAPPS>.
- Hamzah, K., Yasutra, A., & Irawan, D., 2021, Prediction of Hydraulic Fractured Well Performance Using Empirical Correlation and Machine Learning. *Scientific Contributions Oil and Gas*, 44(2), 141–152. <https://doi.org/10.29017/scog.44.2.589>
- Herdiansyah, F., Prakoso, S., Arianto, A., & Badril, A., 2023, Multi-Layer Facies Distribution of Sihapas Group in the Central Region of Central Sumatra Basin. In H. Riswandi, T. Igarashi, C. Tabelin, T. Pasang, O. F. Ugurly, Y. Rizkianto, & O. W. Lusantono (Eds.), *AIP Conference Proceedings* (Vol. 2598). American Institute of Physics Inc. <https://doi.org/10.1063/5.0129125>.
- Ibrahim, S. S., Boulos, T. R., Abdullah, S. M., Elbendari, A. M., Khalifa, M. G., & Hagrass, A. A., 2025. Improving the quality of silica sand as a proppant for hydraulic fracking industry purposes. *Rudarsko Geolosko Naftni Zbornik*, vol. 40 no. 1, pp. 145–163. <https://doi.org/10.17794/rgn.2025.1.11>
- Kamel, A., Salem, Z., Chemini, R., Khodja, M., & Allia, K., 2019, Characterization of natural sand proppant used in hydraulic fracturing fluids. In *Particulate Science and Technology* Vol. 37 no. 6, pp. 716–724). Taylor and Francis Inc. <https://doi.org/10.1080/02726351.2018.143854>
- Khaing, S. Y., Surjono, S. S., Setyowiyoto, J., & Sugai, Y., 2017,. Facies and Reservoir Characteristics of the Ngrayong Sandstone in the Rembang Area, Northeast Java (Indonesia). *Open Journal of Geology*, vol. 7 no. 5, pp. 608–620. <https://doi.org/10.4236/ojg.2017.75042>.

- Khaing, S. Y., Sugai, Y., Tun, M. M., Surjono, S. S., & Setyowiyoto, J, 2022, Textural Characteristics and Depositional Environment of Ngrayong Sandstone (Middle Miocene) from Rembang Area, Northeast Java, Indonesia. *Open Journal of Geology*, vol. 12 no. 12, pp. 1102–1119. <https://doi.org/10.4236/ojg.2022.1212052>.
- Krumbein, W. C., & Sloss, L. L., 1963, *Stratigraphy and sedimentation* (2nd ed.). Freeman. (1963).
- Lam, R. C, 2019, Analysis of crush resistance and Mississippi-sourced sands to Analysis of crush resistance and Mississippi-sourced sands to determine potential as proppant sands determine potential as proppant sands. https://egrove.olemiss.edu/hon_thesis/1065.
- Liu, H., Wang, X., Xu, N., Chen, Z., & Peng, Y, 2024, Research on the transport behavior of microparticle proppants inside natural fractures. *Frontiers in Earth Science*, 12. <https://doi.org/10.3389/feart.2024.1418783>.
- Ngwe, T., Myo Min Swe, M., & Myint Than, M., 2019, Review of the Proppant Selection for Hydraulic Fracturing. In *International Journal of Science and Engineering Applications*, vol. 8. www.ijsea.com418.
- Peng, H., Yang, J., Liu, F., Zhang, X., Ning, F., Peng, H., Liu, Z., Sun, J., Cheng, W., Cui, G., & Shi, P, 2025, The Evaluation Method and Performance Requirements of Quartz Sand for Shale Gas Fracturing. *Energies*, vol. 18 no. 8. <https://doi.org/10.3390/en18081979>.
- R.D. Barree, B. & A. S. A. C. M. O. C. V. L. B. B. & A. M. W. C. S.-L. I, 2003, Realistic Assessment of Proppant Pack Conductivity for Material Selection.
- Richard, S., Schrader, S., Schrader, R., Ereaux, B., & Tech, M, 2019, SPE-195368-MS Improved Methods of Measuring Proppant Conductivity.
- Saaid, I. M., Kamat, D., & Muhammad, S, 2011, Characterization of Malaysian Sand for Possible Use as Proppant. In *American International Journal of Contemporary Research*, vol. 1, no. 1 www.ajcernet.com.
- Syaranamual, E. E., Rahmawati, S. D., & Lumban Gaol, A. H., 2025, New Perspective of Unconventional Hydrocarbon Production With Emission Calculations. *Scientific Contributions Oil and Gas*, 48(3), 113–129. <https://doi.org/10.29017/scog.v48i3.1790>
- Tang, Y., Ranjith, P. G., & Perera, M. S. A, 2018, Major factors influencing proppant behaviour and proppant-associated damage mechanisms during hydraulic fracturing. In *Acta Geotechnica*, vol. 13, no. 4, pp. 757–780). Springer Verlag. <https://doi.org/10.1007/s11440-018-0670-5>
- Tschapek, M., Wasowk-si, C., & Falasca, S, 1983, Character and change in the hydrophilic properties of quartz sand. In *Z. Pflanzenernaehr. Bodenk vol. 146*.
- Wahab Gaber, M. A., A Wahab, M., & El-Din Ibrahim, G. A, 2021a, Characterization of some Egyptian white sand and dunes for utilization as hydraulic fracturing sand for tight oil well layers. In *Annals Geol. Surv. Egypt vol. 38*. <https://www.researchgate.net/publication/345947748>.
- Wahab Gaber, M. A., AWahab, M., & El-Din Ibrahim, G. A, 2021b, Characterization of some Egyptian white sand and dunes for utilization as hydraulic fracturing sand for tight oil well layers. In *Annals Geol. Surv. Egypt vol. 38*. <https://www.researchgate.net/publication/345947748>.
- Wei, J. G., Wang, X. J., Fu, X. F., Gong, P. Q., Zhou, X. F., Li, Y. W., Yang, Y., Chen, Y. H., Jia, B., & Wu, J, 2022, Optimization of long-term fracture conductivity with quartz: An experimental investigation. *Frontiers in Energy Research*, 10. <https://doi.org/10.3389/ferg.2022.973349>.
- Xu, F., Yao, K., Li, D., Xu, D., & Yang, H, 2022, Study on the Effect of Acid Corrosion on Proppant Properties. *Energies*, vol. 15 no. 22 <https://doi.org/10.3390/en15228368>.
- Zoveidavianpoor, M., & Gharibi, A, 2015, Application of polymers for coating of proppant in hydraulic fracturing of subterranean formations: A comprehensive review. In *Journal of Natural Gas Science and Engineering*, vol.

24, pp. 197–209. Elsevier B.V. <https://doi.org/10.1016/j.jngse.2015.03.024>.

Zoveidavianpoor, M., & Gharibi, A, 2016, Characterization of agro-waste resources for potential use as proppant in hydraulic fracturing. *Journal of Natural Gas Science and Engineering*, vol 36, pp. 679–691. <https://doi.org/10.1016/j.jngse.2016.10.045>